Role of the Bridging Arylethynyl Ligand in Bi- and Trinuclear Ruthenium and Iron Complexes

Axel Klein,*[,†] Olivier Lavastre,*[,‡] and Jan Fiedler[§]

Institut für Anorganische Chemie, Universität zu Köln, Greinstrasse 6, D-50939 Köln, Germany, Institut de Chimie CIT Rennes, UMR 6509 CNRS Université de Rennes 1, Campus de Beaulieu, F-35042 Rennes, France, and J. Heyrovský Institute of Physical Chemistry, Academy of Sciences of the Czech Republic, Dolejškova 3, CZ-18223 Prague, Czech Republic

Received October 11, 2005

A series of binuclear homometallic complexes [M−(μ-L)−M] containing ruthenium (M = [−Ru(dppe)$_2$Cl], dppe = 1,2-bis(diphenylphosphino)ethane) and iron (M = [−C_5H_4−Fe−C_5H_5] = ferrocenyl) and trinuclear heterobimetallic complexes [M−(μ-L)−M′−(μ-L)−M] (M′ = [Pd(P^nBu_3)$_2$], [Ru(dppe)$_2$]) in which the metals are bridged by arylethynyl ligands (μ-L = −C≡C{(*p*-C_6H_4)C≡C}$_n$−) of various lengths (n = 1−3) was prepared and investigated, focusing on their electrochemical behavior. Depending on the length and nature of the bridge the coupling of the fully reversible electrochemical oxidations varies from strong to zero. The comproportionation constant K_C and hence the stability of the intermediate mixed-valent species is discussed in view of the nature of the bridge and compared to related systems with other types of unsaturated carbon ligands. The character of the oxidized states was examined using spectroelectrochemical techniques (UV/vis/near-IR, IR, or EPR) with special focus on the intervalence charge-transfer band (IVCT) of the mixed-valent monocations and the EPR behavior. Since the IVCT bands could not be assigned unequivocally and the EPR reveals marked alkynyl ligand contribution to the oxidized state for the ruthenium complexes, an alternative assignment (intraligand transitions) for the long-wavelength bands is discussed.

Introduction

Aryldiethynyls, −C≡C(Ar)C≡C−, together with other unsaturated carbon ligands such as alkynyls, arylethynyls, arylethenyls, and cumulenes[1−10] are of great interest in the organometallic chemistry of transition metals. This is due to their electronically unsaturated nature, which confers to such compounds a number of interesting properties and applications such as (i) reversible redox chemistry,[2a,b,g,l,m,3,6i] (ii) easily accessible mixed-valent states in binuclear complexes,[2c,g,k,m] (iii) liquid crystalline behavior,[11] (iv) luminescence,[3,5a,c,d,f,6b,c,f,i] (v) third-order nonlinear optical materials,[1,2e,4f,12] and molecular electronics.[2c,5b,6h,7,13] The prevailing use of the aryldiethynyl group lies in bridging two or more transition metals to form binuclear or oligonuclear complexes which extend to the interesting field of organometallic polymers.[4e,5a,b,e,f,6]

If the chosen metals exhibit reversible redox couples such as, for example, M(II)/M(III), iron or ruthenium binuclear complexes with arylethynyl bridging ligands usually allow the

* To whom correspondence should be addressed. E-mail: axel.klein@uni-koeln.de (A.K.); olivier.lavastre@univ-rennes1.fr (O.L.).

† Universität zu Köln.

‡ UMR 6509 CNRS Université de Rennes 1.

§ Academy of Sciences of the Czech Republic.

(1) For a recent review on metal−alkynyl complexes see: Long, N. J.; Williams, C. K. *Angew. Chem., Int. Ed*. **2003**, *42*, 2586−2617.

(2) *Binuclear homometallic systems with aryldiethynyl bridges*: (a) De Montigny, F.; Argouarch, G.; Costuas, K.; Halet, J.-F.; Roisnel, T.; Toupet, L.; Lapinte, C. *Organometallics* **2005**, *24*, 4558−4572. (b) Chawdhury, N.; Long, N. J.; Mahon, M. F.; Ooi, L.-L.; Raithby, P. R.; Rooke, S.; White, A. J. P.; Williams, D. J.; Younus, D. M. *J. Organomet. Chem*. **2004**, *689*, 840−847. (c) Fraysse, S.; Coudret, C.; Launay, J.-P. *J. Am. Chem. Soc.* **2003**, *125*, 5880−5888. (d) Callejas-Gaspar, B.; Laubender, M.; Werner, H. *J. Organomet. Chem*. **2003**, *684*, 144−152. (e) Hurst, S. K.; Cifuentes, M. P.; McDonagh, A. M.; Humphrey, M. G.; Samoc, M.; Luther-Davies, B.; Asselberghs, I.; Persoons, A. *J. Organomet. Chem*. **2002**, *642*, 259−267. (f) Albertin, G.; Agnoletto, P.; Antoniutti, S. *Polyhedron* **2002**, *21*, 1755−1760. (g) Hurst, S. K.; Ren, T. *J. Organomet. Chem*. **2002**, *660*, 1−5. (h) Back, S.; Lutz, M.; Spek, A. L.; Lang, H.; Van Koten, G. *J. Organomet. Chem*. **2001**, *620*, 227−234. (i) Albertin, G.; Antoniutti, S.; Bordignon, E.; Granzotto, M. *J. Organomet. Chem.* **1999**, *585*, 83−92. (j) Bruce, M. I.; Hall, B. C.; Kelly, B. D.; Low, P. J.; Skelton, B. W.; White, A. H. *J. Chem. Soc., Dalton Trans*. **1999**, 3719−3728. (k) Colbert, M. C. B.; Lewis, J.; Long, N. J.; Raithby, P. R.; Younus, M.; White, A. J. P.; Williams, D. J.; Payne, N. N.; Yellowlees, L.; Beljonne, D.; Chawdhury, N.; Friend, R. H. *Organometallics* **1998**, *17*, 3034−3043. (l) Duffy, N.; McAdam, J.; Nervi, C.; Osella, D.; Ravera, M.; Robinson, B.; Simpson, J. *Inorg. Chim. Acta* **1996**, *247*, 99−104. (m) Field, L. D.; George, A. V.; Laschi, F.; Malouf, E. Y.; Zanello, P. *J. Organomet. Chem.* **1992**, *435*, 347−356.

(3) *Heterobimetallic systems with aryldiethynyl bridges*: Wong, K. M.-C.; Lam, S. C.-F.; Ko, C.-C.; Zhu, N.; Yam, V. W.-W.; Roue, S.; Lapinte, C.; Fathallah, S.; Costuas, K.; Kahlal, S.; Halet, J.-F. *Inorg. Chem*. **2003**, *42*, 7086−7097.

(4) *Oligonuclear systems with aryldiethynyl bridges*: (a) Vicente, J.; Chicote, M.-T.; Alvarez-Falcon, M. M.; Jones, P. G. *Organometallics* **2005**, *24*, 2764−2772. (b) Albinati, A.; Leoni, P.; Marchetti, L.; Rizzato, S. *Angew. Chem., Int. Ed*. **2003** *42*, 5990−5993. (c) Chin, C. S.; Kim, M.; Won, G.; Jung, H.; Lee, H. *Dalton Trans*. **2003**, 2325−2328. (d) Chin, C. S.; Kim, M.; Lee, H.; Noh, S.; Ok, K. M. *Organometallics* **2002**, *21*, 4785−4793. (e) Bruce, M. I.; Davy, J.; Hall, B. C.; Van Galen, Y. J.; Skelton, B. W.; White, A. H. *Appl. Organomet. Chem.* **2002**, *16*, 559−568. (f) Weyland, T.; Ledoux, I.; Brasselet, S.; Zyss, J.; Lapinte, C. *Organometallics* **2000**, *19*, 5235−5237. (g) Lavastre, O.; Plass, J.; Bachmann, P.; Guesmi, S.; Moinet, C.; Dixneuf, P. H. *Organometallics* **1997**, *16*, 184−189.

(5) *Extended arylethynyl ligands*: (a) Liu, Y.; Jiang, S.; Schanze, K. S. *Chem. Commun*. **2003**, 650−651. (b) Hortholary, C.; Coudret, C. *J. Org. Chem*. **2003**, *68*, 2167−2174. (c) Chao, H.-Y.; Lu, W.; Li, Y.; Chan, M. C. W.; Che, C.-M.; Cheung, K.-K.; Zhu, N. *J. Am. Chem. Soc*. **2002**, *124*, 14696−14706. (d) Walters, K. A.; Ley, K. D.; Cavalaheiro, C. S. P.; Miller, S. E.; Gosztola, D.; Wasielewski, M. R.; Bussandri, A. P.; Van Willigen, H.; Schanze, K. S. *J. Am. Chem. Soc*. **2001**, *123*, 8329−8342. (e) Khan, M. S.; Kakkar, A. K.; Ingham, S. L.; Raithby, P. R.; Lewis, J.; Spencer, B.; Wittmann, F.; Friend, R. H. *J. Organomet. Chem*. **1994**, *472*, 247−255. (f) Khan, M. S.; Kakkar, A. K.; Long, N. J.; Lewis, J.; Raithby, P. R.; Nguyen, P.; Marder, T. B.; Wittmann, F.; Friend, R. H. *J. Mater. Chem*. **1994**, *4*, 1227−1232.

10.1021/om050876k CCC: $33.50
Publication on Web 12/21/2005

generation of mixed-valence species and the study of intramolecular electron transfer (ET) in such mixed-valence systems. The study of ET through mixed-valence compounds is a very active field of research. A large number of compounds have been synthesized, allowing the study of various factors such as the distance of the redox centers, solvent effects, and the nature of the bridging ligand.[14] The effectiveness of the ET process is related to the stability of the mixed-valence state and can be discussed on the basis of the comproportionation constant K_C (eq 1; for the reaction $M^n + M^{(n-2)} \rightleftarrows 2M^{(n-1)}$ at 25 °C), which

$$K_C = 10^{\Delta E/59\text{mV}} = [M^{(n-1)}]^2/[M^n][M^{(n-2)}] \qquad (1)$$

can be measured directly electrochemically. Furthermore, the appearance of the intervalence transition (IVCT) is a measure for the effectivity of the ET process, according to the Hush relation (eq 2).[15] Full inspection of the IVCT band yields the electronic coupling parameter V_{ab} describing the amount of

$$\nu_{max} - \nu_0 = (\Delta\nu_{1/2})^2/2310\ \text{cm}^{-1} \qquad (2)$$

ν_{max} = transition energy in cm^{-1},

$\Delta\nu_{1/2}$ = full width at half-height in cm^{-1},

ν_0 = change of free energy ΔG in cm^{-1}

electronic interaction between remote sites and the distance r of the redox centers (eq 3).[2k,8h,15] From this interaction, general

$$V_{ab} = (2.05 \times 10^{-2}/r)(\epsilon_{max}\nu_{max}\Delta\nu_{1/2})^{1/2} \qquad (3)$$

ϵ in L mol^{-1} cm^{-1}, r = distance of the redox centers in Å

rules for the design of efficient bridging ligands allowing long-distance electron transfer have been derived.[14]

Aryldiethynyl bridging ligands are ideally suited to learn how the ET depends on the (electronic) structure of such bridges. The aryl core can be varied to a great extent by replacing the common 1,4-phenylene, for example, by 1,3-phenylene,[2a,f,j,4f] 2,5-pyridine,[2b,k] 2,5-thiophene,[2a−c,k,4e,5f,6i] 9,10-anthracene,[2a−c,4e,5f] or 4,4′-biphenylene.[2b,e,5c,f] Further promising variations are the prolongation of the chain length to bis(aryldiethynyl), tris(aryldiethynyl), etc. or the incorporation of metals into such extended systems. The extension of the unsaturated carbon chain which is very common for cummulenes,[2a,8f,9a,b] for example, has been so far restricted for aryldiethynyl complexes to only a few cases of mononuclear ruthenium systems,[5a−c] a binuclear gold system,[5c] and some polymeric platinum systems.[5f,6b−f] A study on the ET properties of such extended ligands has not been reported so far. Studies on the incorporation of metals into the chain to form trinuclear [M]−C≡C(Ar)C≡C−[M′]−C≡C(Ar)C≡C−[M][4g] or oligonuclear systems[6j] have so far been restricted to synthetic details. ET studies on related acetylide-bridged heterotrinuclear systems with ferrocene end groups have been reported recently.[1,16]

In this paper we wish to report our investigation on a series of binuclear homometallic complexes [M−(μ-L)−M] (**A** in Chart 1) and trinuclear complexes [M−(μ-L)−M′−(μ-L)−M] (**B**) (M′ = [Pd(P^nBu_3)$_2$], [Ru(dppe)$_2$]; dppe = 1,2-bis(diphenylphosphino)ethane) where metals separate an aryldiethynyl chain (μ-L) linking two redox-active ruthenium (M = [−Ru(dppe)$_2$Cl]; **Ru** in Chart 2) or iron centers (M = [−C_5H_4−Fe−C_5H_5] (ferrocenyl; **Fc** in Chart 2). By learning how the ET properties depend on the length of the bridge, the metal terminus, and the incorporated metal linker (see Scheme 1) we want to

(6) *Metallo-polymeric systems with arylethynyl ligands*: (a) Köhler, A.; Beljonne, D. *Adv. Funct. Mater*. **2004**, *14*, 11−18. (b) Wong, W.-Y.; Wong, C.-K.; Lu, G.-L.; Lee, A. W.-M.; Cheah, K.-W.; Shi, J.-X. *Macromolecules* **2003**, *36*, 983−990. (c) Fradotti, I.; Battocchio, C.; Furlani, A.; Mataloni, P.; Polzonetti, G.; Russo, M. V. *J. Organomet. Chem.* **2003**, *674*, 10−23. (d) La Groia, A.; Ricci, A.; Bassetti, M.; Masi, D.; Bianchini, C.; Lo Sterzo, C. *J. Organomet. Chem*. **2003**, *783*, 406−420. (e) Long, N. J.; White, A. J. P.; Williams, D. J.; Younus, M. *J. Organomet. Chem*. **2002**, *649*, 94−99. (f) Liu, Y.; Jiang, S.; Glusac, K.; Powell, D. H.; Anderson, D. F.; Schanze, K. S. *J. Am. Chem. Soc.* **2002**, *124*, 12412−12413. (g) Matsumi, N.; Chujo, Y.; Lavastre, O.; Dixneuf, P. H. *Organometallics* **2001**, *20*, 2425−2427. (h) Creager, S.; Yu, C. J.; Bamdad, C.; O'Connor, S.; MacLean, T.; Lam, E.; Chong, Y.; Olson, G. T.; Luo, J.; Gozin, M.; Kayyem, J. F. *J. Am. Chem. Soc*. **1999**, *121*, 1059−1064. (i) Younus, M.; Köhler, A.; Cron, S.; Chawdhury, N.; Al-Mandhary, M. R. A.; Khan, M. S.; Lewis, J.; Long, N. J.; Friend, R. H.; Raithby, P. R. *Angew. Chem*. **1998**, *110*, 3180−3183. (j) Lavastre, O.; Even, M.; Dixneuf, P. H.; Pacreau, A.; Vairon, J.-P. *Organometallics* **1996**, *15*, 1530−1531.

(7) *Arylethynyl polymers and materials*: (a) Stroh, C.; Mayor, M.; Von Hänisch, C.; Turek, P. *Chem. Commun*. **2004**, 2−4. (b) Weber, H. B.; Mayor, M. *Phys. Unserer Zeit* **2003**, *34*, 272−278. (c) Sirota, M.; Fradkin, L.; Buller, R.; Henzel, V.; Lahav, M.; Lifshitz, E. *Chem. Phys. Chem*. **2002**, *3*, 343−349. (d) Hensel, V.; Godt, A.; Popovitz-Biro, R.; Cohen, H.; Jensen, T. R.; Kjaer, K.; Weissbuch, I.; Lifshitz, E.; Lahav, M. *Chem. Eur. J*. **2002**, *8*, 1413−1423.

(8) *Systems with alkynyl bridges*: (a) Venkatesan, K.; Fox, T.; Schmalle, H. W.; Berke, H. *Organometallics* **2005**, *24*, 2834−2847. (b) Bruce, M. I.; Ellis, B. G.; Low, P. J.; Skelton, B. W.; White, A. H. *Organometallics* **2003**, *22*, 3184−3198. (c) Hoshino, Y.; Higuchi, S.; Fiedler, J.; Su, C.-Y.; Knödler, A.; Schwederski, B.; Sarkar, B.; Hartmann, H.; Kaim, W. *Angew. Chem., Int. Ed.* **2003**, *42*, 674−677. (d) Bruce, M. I.; Low, P. J.; Costuas, K.; Halet, J.-F.; Best, S. P.; Heath, G. A. *J. Am. Chem. Soc*. **2000**, *122*, 1949−1962. (e) Paul, F.; Meyer, W. E.; Toupet, L.; Jiao, J.; Gladysz, J. A.; Lapinte, C. *J. Am. Chem. Soc.* **2000**, *122*, 9405−9414. (f) Dembinski, R.; Bartik, T.; Bartik, B.; Jaeger, M.; Gladysz, J. A. *J. Am. Chem. Soc*. **2000**, *122*, 810−822. (g) Guillemot, M.; Toupet, L.; Lapinte, C. *Organometallics* **1998**, *17*, 1928−1930. (h) Coat, F.; Guillevic, M.-A.; Toupet, L.; Paul, F.; Lapinte, C. *Organometallics* **1997**, *16*, 5988−5998. (i) Brady, M.; Weng, W.; Zhou, Y.; Seyler, J. W.; Amoroso, A. J.; Arif, A. M.; Böhme, M.; Frenking, G.; Gladysz, J. A. *J. Am. Chem. Soc.* **1997**, *119*, 775−788. (j) Le Narvor, N.; Toupet, L.; Lapinte, C. *J. Am. Chem. Soc.* **1995**, *117*, 7129−7138.

(9) *Metallacumulenes as bridges*: (a) Skibar, W.; Kopacka, H.; Wurst, K.; Salzmann, C.; Ongania, K.-H.; Fabrizi de Biani, F.; Zanello, P.; Bildstein, B. *Organometallics* **2004**, *23*, 1024−1041. (b) Touchard, D.; Dixneuf, P. H. *Coord. Chem. Rev.* **1998**, *178−180*, 409−429. (c) Paul, F.; Lapinte, C. *Coord. Chem. Rev.* **1998**, *178−180*, 431−509. (d) Guesmi, S.; Touchard, D.; Dixneuf, P. H. *J. Chem. Soc., Chem. Commun.* **1996**, 2773−2774.

(10) *Arylethenyls as bridges:* Mata, J. A.; Peris, E.; Llusar, R.; Uriel, S.; Cifuentes, M. P.; Humphrey, M. G.; Samoc, M.; Luther-Davies, B. *Eur. J. Inorg. Chem.* **2001**, 2113−2122.

(11) (a) Fischer, M.; Lieser, G.; Rapp, A.; Schnell, I.; Mamdouh, W.; De Feyter, S.; De Schryver, F. C.; Hoeger, S. *J. Am. Chem. Soc*. **2004**, *126*, 214−222. (b) Bunz, U. H. F. *NATO ASI Ser., Ser. C* **1997**, *499*, 473−484. (c) Bunz, U. H. F. *Top. Curr. Chem.* **1999**, *201*, 131−161.

(12) (a) Fillaut, J.-L.; Perruchon, J.; Blanchard, P.; Roncali, J.; Golhen, S.; Allain, M.; Migalsaka-Zalas, A.; Kityk, I. V.; Sahraoui, B. *Organometallics* **2005**, *24*, 687−695. (b) Long, N. J. *Angew. Chem., Int. Ed. Engl*. **1995**, *34*, 21−38. (c) Blau, W. J.; Byrne, H. J.; Cardin, D. J.; Davey, A. P. In *Organic Molecules for Nonlinear Optics and Photonics*; Messier, J., Kajar, F., Prasad, P., Ulrich, D., Eds.; Kluwer Academic: Dordrecht, The Netherlands, 1991; p 391.

(13) (a) Chen, J.; Reed, M. A.; Rawlett, A. M.; Tour, J. M. *Science* **1999**, *286*, 1550−1552. (b) Hu, W.; Nakashima, H.; Furukawa, K.; Kashimura, Y.; Ajito, K.; Torimitsu, K. *Appl. Phys. Lett.* **2004**, *85*, 115−117. (c) Zhitenev, N. B.; Erbe, A.; Bao, Z. *Phys. Rev. Lett.* **2004**, *92*, 186805/1−186805/4. (d) Park, J.; Pasupathy, A. N.; Goldsmith, J. I.; Chang, C.; Yaish, Y.; Petta, J. R.; Rinkoski, M.; Sethna, J. P.; Abruna, H. D.; McEven, P. L.; Ralph, D. C. *Nature* **2002**, *417*, 722−725.

(14) *Some reviews on intramolecular electron transfer in mixed-valence systems*: (a) Brunschwig, B. S.; Creutz, C.; Sutin, N. *Chem. Soc. Rev.* **2002**, *31*, 168−184. (b) Nelsen, S. F. In *Electron Transfer in Chemistry*; Balzani, V., Ed.; Wiley-VCH: Weinheim, Germany, 2001; Vol. 1, Chapter 10. (c) Launay, J.-P.; Coudret, C. In ref 14b, Vol. 5, Chapter 1. (d) Demadis, K. D.; Hartshorn, C. M.; Meyer, T. J. *Chem. Rev*. **2001**, *101*, 2655−2685. (e) Kaim, W.; Klein, A.; Glöckle, M. *Acc. Chem. Res.* **2000**, *33*, 755−763.

(15) Hush, N. S. *Prog. Inorg. Chem*. **1967**, *8*, 391−444.

(16) (a) Zhu, Y.; Clot, O.; Wolf, M. O.; Yap, G. P. A. *J. Am. Chem. Soc*. **1998**, *120*, 1812−1821. (b) Colbert, M. C. B.; Lewis, J.; Long, N. J.; Raithby, P. R.; White, A. J. P.; Williams, D. J. *J. Chem. Soc., Dalton Trans*. **1997**, 99−104.

Chart 1. Schematic Representation of Bi- and Trimetallic Models A and B and of Homo- and Heterometallic Conjugated Polymers C

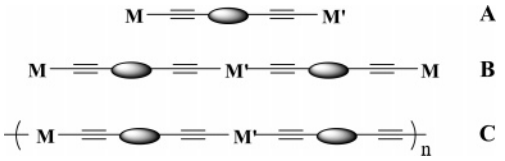

Scheme 1. Variations for the ET System Used in This Study[a]

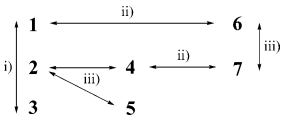

[a] Legend: (i) the length of the bridge; (ii) the metal termini; (iii) the presence of organometallic linkers.

approach the interesting aim of heterometallic conjugated metallo polymers (**C**).[6g]

Results and Discussion

Synthesis of the Complexes. The synthesis of the complexes **1**, **4**, **6**, and **7** has been described previously;[4g] the preparation of **2**, **3**, and **5**, which follows established methods,[1,4g,6j] is summarized in Scheme 2. Details can be found in the Experimental Section.

Electrochemistry. The complexes **1**, **2**, and **4** show two reversible, clearly separated one-electron-oxidation steps followed by a third irreversible oxidation (see Table 1). The separations of the first two waves given in Table 1 were determined by square-wave voltammetry and simulation of the CV curves. For the trinuclear complex **5** the situation is slightly different. Quantitative measurements using the Baranski method[17] revealed that the second wave consists of two electrons. Assuming mainly ruthenium-centered oxidations (Ru(II)/Ru(III)) and expecting higher electron density at the central Ru(II) atom, we conclude that the first oxidation occurs at the latter and the two successive steps are then due to the oxidation of the two peripheral Ru(II) centers. Whether these two steps are separated or not, cannot be determined directly from electro-

Chart 2. Variety of Organic and Organometallic Wires with Numbering of the Presented Compounds

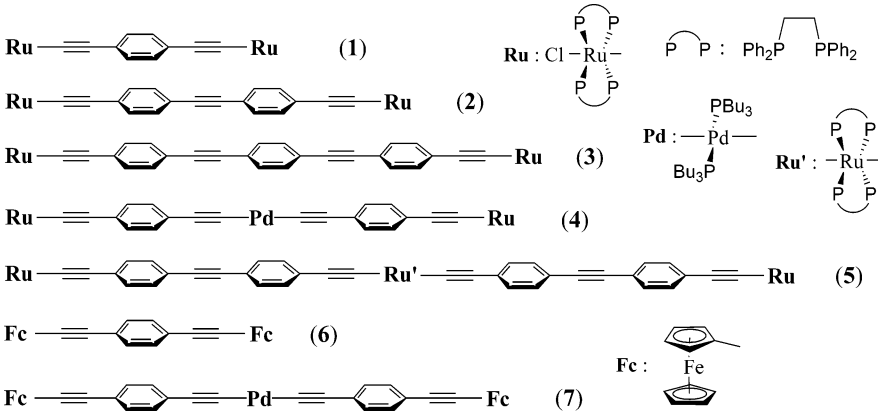

Scheme 2. Synthesis of Derivatives 2, 3, and 5 Using Metal−Carbon Bond Formation or Catalytic Carbon−Carbon Bond Formation

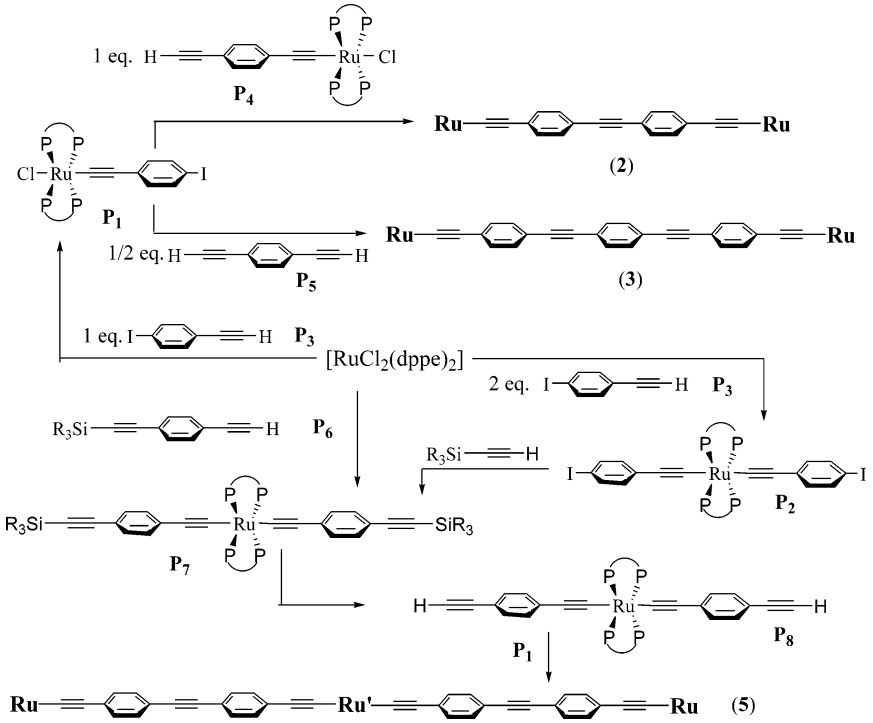

Table 1. Electrochemical Data of Binuclear Ruthenium and Iron Complexes[a]

compd	$E_{p,a}$(Ox3)	$E_{1/2}$(Ox2) (ΔE_{pp})	$E_{1/2}$(Ox1) (ΔE_{pp})	$\Delta(E°(\text{Ox2}) - E°(\text{Ox1}))^b$	$K_C{}^b$
1	0.96 irr	0.013 (65) [1.0]	−0.328 (61) [1.0]	341	6.0×10^5
2	0.84 irr	0.035 (78) [0.99]	−0.026 (78) [1.0]	61	10.8
3	0.80 irr		−0.002 (82) [1.9]		
4	0.62 irr	−0.006 (93) [0.96]	−0.134 (75) [1.0]	128	147.7
5	0.77 irr	0.014 (87) [1.85]	−0.036 (78) [1.0]	50	7.0
6	1.20 irr		0.56 (86)[1.87]		
7	1.07 irr		0.55 (75) [1.83]		

[a] From cyclic or square-wave voltammetry in 0.1 M $CH_2Cl_2/{}^nBu_4NPF_6$ solutions at 100 mV/s scan rate. Potentials $E_{1/2}$ are in V vs $FeCp_2^{0/+}$, peak potential differences ΔE_{pp} are in mV, and numbers of electrons are in F/mol (given in square brackets) (see text). Anodic peak potentials $E_{p,a}$ are in V for irreversible oxidation steps. [b] Error margins = ±0.5 mV for all $\Delta(E°(\text{Ox2}) - E°(\text{Ox1}))$. For **1** this calculates to $\pm 0.12 \times 10^5$ for K_C.

chemical experiments. Simulation allows us to give a maximum separation of 15 mV, but in view of the other results we do not assume any coupling. For **3**, **6**, and **7** only one reversible oxidation wave is observed, which contains ca. 1.9 electrons as determined by quantitative measurements. However, these waves should be considered as two coinciding one-electron waves due to noncoupling of the two individual redox processes at each metal center.

The comproportionation constants K_C derived from eq 1 for the mixed-valence species are calculated to be 6×10^5 for $[\mathbf{1}]^+$, only about 150 for $[\mathbf{4}]^+$, and very small for $[\mathbf{2}]^+$ (10) and $[\mathbf{5}]^+$ or $[\mathbf{5}]^{2+}$ (7 or 1.8, respectively). With increasing chain length on going from $[\mathbf{1}]^+$ to $[\mathbf{3}]^+$ the stability of the mixed-valence state decreases sharply to zero for $[\mathbf{3}]^+$. Comparing the palladium-bridged complex **4** with an appreciable separation of ca. 130 mV ($K_C \approx 150$) with **3** reveals that the palladium linker provides some beneficial properties; the slightly decreased chain length on replacing 1,4-phenylene with Pd cannot account for this effect. Recently Mayor et al. have concluded from EPR measurements that corresponding $\{Pt(PPh_3)_2\}$ units allow effective electronic coupling in related arylethynyl systems. Contributions from the platinum d orbitals were quoted as a possible explanation.[7a] Our results seem to support this assumption. Comparing the trinuclear complex **5** with binuclear **2** (both contain the same arylethynyl ligand) reveals a slightly reduced K_C for the first oxidation product of **5** [Ru(II)−(μ-L)−Ru′(III)−(μ-L)−Ru(II)]. These differences are due to the altered character for the metal fragment, which has a strong impact on the ET properties, as we can see from comparison to the ferrocenyl systems described below and related systems.

Long et al. have reported a K_C value for $[\{ClRu(dppm)_2\}_2(\mu\text{-}L^1)]^+$ (μ-L^1 = −C≡CC$_6$H$_4$C≡C−) of 1.2×10^5,[2k] which reveals already the effect of replacement of the dppm by the dppe coligand. Changing 1,4-phenylene to 2,5-thiophene increased K_C to 1.2×10^6; introducing the unfavorable 1,3-phenylene gave a sharply decreased value of 1.6×10^3. Much better coupling is observed in C_4-alkynyl systems [M−C≡CC≡C−M] such as [Cp*Fe(dippe)] ($K_C = 2.25 \times 10^{13}$, dippe = ethylenebis(diisopropylphosphine)[8b,g] and $[CpRu(PPh_3)_2]$ ($K_C = 1.5 \times 10^{11}$).[8b,d] However, an adequate comparison of the two different systems would be with C_8-alkynyl-bridged systems [M−C≡CC≡CC≡CC≡C−M]. Both C_4 and C_8 systems have been investigated for M = [Cp*Re(PPh$_3$)(NO)] by Gladysz et al. The study reveals that K_C value decreases dramatically from C_4 (1.1×10^9) to C_8 (5.9×10^4).[8f] The above comparison is furthermore lacking, due to the fact that in the aforementioned C_4-alkynyl systems the electron-rich Cp or Cp* coligand enhanced markedly the stability of the mixed-valence state.[18]

Replacing ruthenium in analogous complexes by iron seems to results in markedly decreased K_C values. For example, a K_C value of 2.4×10^3 was found for $[\{ClFe(dmpe)_2\}_2(\mu\text{-}L^1)]$ (dmpe = 1,2-bis(dimethylphosphino)ethane)[2m] and a value of 5.1×10^2 was determined for $[\{ClFe(depe)_2\}_2(\mu\text{-}L^1)]^+$ (depe = 1,2-bis(diethylphosphino)ethane)[2k] which both can be regarded as iron analogues of **1**. Interestingly, more electron rich iron centers such as, for example, $\{Cp^*Fe(dppe)_2\}$ exhibit higher K_C values. For $[\{Cp^*Fe(dppe)_2\}(\mu\text{-}L^1)]$ a K_C value of 2.6×10^4 was reported.[2a] Introducing an 9,10-anthracenyl−diethynyl bridge in the same system leads to a greatly enhanced K_C value of 2.3×10^6.[2a] A further comparison from the related C_4-alkynyl systems [M−C≡CC≡C−M] reveals that on going from the system M = [−Fe(Cp*)(dppe)],[8b,d,g,k] in which the bridge is directly bound to the metal, to the system [−Cp*−Fe−Cp*],[19] in which the bridge is bound to the Cp coligand reduces K_C from 1.6×10^{12} to 350. Therefore, it is not unexpected that in our ferrocenyl systems the coupling of the two redox processes has vanished. Recent work by Zanello and Bildstein has shown that [4]cumulene-bridged ferrocenyl systems show very effective coupling: e.g. $K_C = 2.6 \times 10^6$ for [Fc(Ph)C=C=C=C(Ph)-Fc].[9a] For the ferrocenyl system the cumulenes seem to be superior to alkynyl or arylethynyl systems.

UV/Vis/Near-IR Spectroscopy. The parent complexes all exhibit long-wavelength transitions of medium to strong intensity (ϵ = 4000−11 000 M^{-1} cm^{-1}) at about 400 nm, which renders all the compounds yellow or orange. In the series of the binuclear ruthenium complexes the long-wavelength absorption energy decreases along the series **1** > **2** > **3** (Table 2). The lowest energy and highest intensity in all of the complexes are found for trinuclear **5**. Both findings agree with an assignment of these bands to a metal (d_{Ru}) to ligand ($\pi^*_{alkynyl}$) charge transfer transition (MLCT). There are further very strong high-energy bands at around 250 nm that very probably correspond to intraligand ($\pi-\pi^*$ or IL) transitions, either within the alkynyl ligands or, less likely, within the phosphine coligands.[20] Recent spectroscopic and quantum-chemical investigations have shown that the highest occupied molecular orbitals (HOMOs) in such complexes obtain strong to main contributions from ligand π orbitals.[2a,c,3,8d,20−22] Therefore, intraligand $\pi-\pi^*$ contributions might be admixed with the long-wavelength MLCT transitions (IL/MLCT) in the present complexes.

Long-wavelength CT bands can be also detected for the ferrocenyl derivatives **6** and **7** at around 330 nm.[23] Additional

(17) Baranski, A. S.; Fawcett, W. R.; Gilbert, C. M. *Anal. Chem.* **1985**, *57*, 166−170.

(18) Chung, M.-C.; Gu, X.; Etzenhouser, B. A.; Spuches, A. M.; Rye, P. T.; Seetharaman, S. K.; Rose, D. J.; Zubieta, J.; Sponsler, M. B. *Organometallics* **2003**, *22*, 3485−3494.

(19) Jutzi, P.; Kleinebekel, B. *J. Organomet. Chem.* **1997**, *545*−*546*, 573−576.

(20) (a) Van Slageren, J.; Winter, R. F.; Klein, A.; Hartmann, S. *J. Organomet. Chem.* **2003**, *670*, 137−143. (b) Winter, R. F.; Klinkhammer, K.-W.; Záliхf0, S. *Organometallics* **2001**, *20*, 1317−1333.

(21) Maurer, J.; Winter, R. F.; Sarkar, B.; Fiedler, J.; Záliхf0, S. *Chem. Commun.* **2004**, 1900−1901.

(22) Yang, L.; Ren, A.-M.; Feng, J.-K.; Liu, X.-D.; Ma, Y.-G.; Zhang, H.-X. *Inorg. Chem.* **2004**, *43*, 5961−5972.

Table 2. Long-Wavelength Absorption Maxima of Binuclear Ruthenium and Iron Complexes[a]

compd	λ_{max} (ϵ)			
[**1**][b]	245 (9.1)	276 (3.1)	356 sh (3.1), 370 (4.4)	
[**1**]$^{\bullet+}$ [b]	268 (2.6)	490 (2.9)	535 (3.5)	1244 sh (2.1), 1526 (3.8), 1889 sh (0.3)
[**1**]$^{2+}$ [b]	278 (4.5)	500 sh (0.7)	620 (2.1)	788 (6.0), 1170 (1.0)
[**2**][c]	249 (10.3)	395 sh (3.6)	420 (4.1)	
[**2**]$^{\bullet+}$ [c]		419 (2.8)	532 (0.8)	879 (0.5), 1700 (0.6), 3260 sh (0.2)
[**2**]$^{2+}$ [c]		383 (2.2)	682 (0.7)	914 (2.3), 1086 sh (1.1)
[**2**]$^{3+}$ [c]	364 (1.9)	455 sh (0.5)	560 sh (0.2)	910 (0.5), 1122 sh (0.3)
[**3**][b]	263 (11.2)	320 (3.8)	428 (6.2)	
[**3**]$^{2+}$ [b,d]	272 (4.1)	354 (5.3)	466 (2.8), 666 (0.3)	909 (2.1)
[**4**][c]	252 (10.8)	286 sh (3.9)	371 (7.2)	
[**4**]$^{\bullet+}$ [c]		368 (4.3)	535 (0.4)	1225 sh (0.2), 1497 (0.7), 1972 sh (0.1)
[**4**]$^{2+}$ [c]		471 (3.8)	665 (0.6)	1003 (3.5), 1542 sh (0.3)
[**4**]$^{3+}$ [c]	356 (2.0)		621 sh (0.4)	801 (0.7)
[**5**][c]	249 (13.8)	305 sh	405 sh, 427 (11.2)	
[**5**]$^{\bullet+}$ [c]	252 (14.8)	333 (5.7)	424 (8.0), 527 sh (1.1)	920 (0.3), 1768 (1.0), 3720 sh (0.1)
[**5**]$^{2+}$ [c]	263 (13.9)	399 (5.2),	418 (5.2), 519 sh	926 (1.3), 1267 (1.8), 1781 (1.4)
[**5**]$^{3+}$ [c]	270 (13.8)	375 (5.7),	454 (2.9), 500 sh (2.1)	953 (2.3), 1274 (3.0)
[**6**][b]	278	323, 357 sh	442	
[**6**]$^{2+}$ [b,d]	269 sh	293	360	556, 789
[**7**][b]	328 sh	338	438	
[**7**]$^{2+}$ [b,d]	271 sh	313	401 sh, 464 sh	576 sh, 891

[a] Generated by electrolysis in 0.1M $^{n}Bu_4NPF_6$/solvent solution; absorption maxima are given in nm, and extinction coefficients ϵ are given in 1000 M^{-1} cm^{-1} (in parentheses). [b] Measured in THF. [c] Measured in CH_2Cl_2. [d] The mixed-valent form []$^{\bullet+}$ could not be detected.

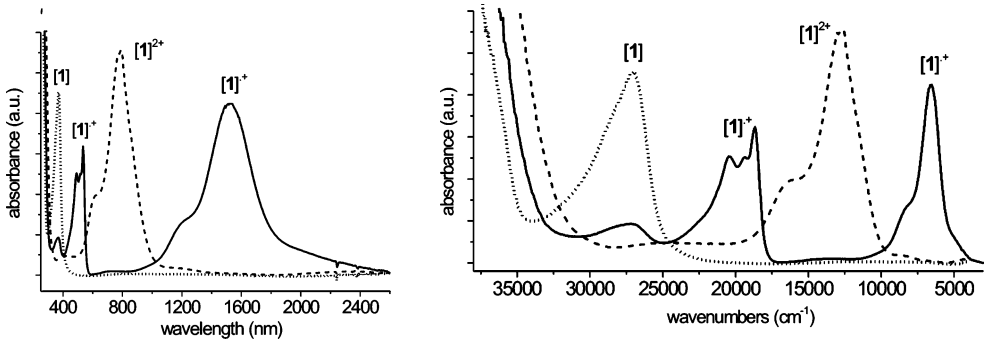

Figure 1. Absorption spectra of [**1**] (dotted line), mixed-valent [**1**]$^{\bullet+}$ (solid line), and [**1**]$^{2+}$ (dashed line), generated in DMF/$^{n}Bu_4NPF_6$.

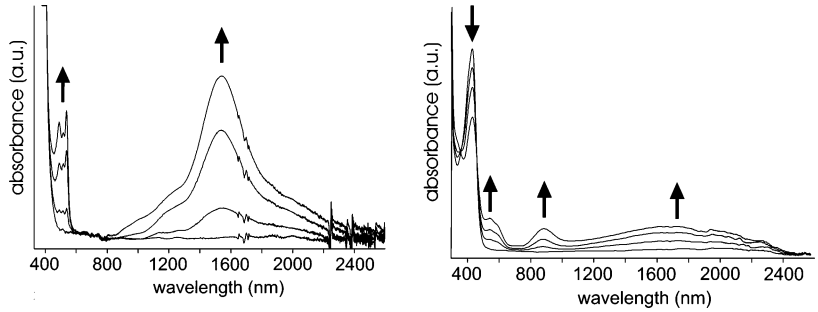

Figure 2. Absorption spectra of [**4**] (left) and [**2**] (right) taken during the electrochemical oxidation in THF/$^{n}Bu_4NPF_6$.

weak bands are observed at slightly lower energy (~440 nm), which are assigned to ligand-field transitions, since they also occur in ferrocene (443 and 321 nm).[24]

UV/Vis/Near-IR Spectroelectrochemistry. After the first oxidation of the ruthenium derivatives **1** and **4** broad bands between 1500 and 1800 nm are discernible that might be assigned to intervalence charge transfer (IVCT) transitions for the complexes [**1**]$^{\bullet+}$ (1526 nm (ϵ = 3800 M^{-1} cm^{-1})) and [**4**]$^{\bullet+}$ (1497 nm (600)) (Figures 1 and 2). However, there are also long-wavelength bands for [**2**]$^{\bullet+}$ at 1700 nm (600) and for [**5**]$^{\bullet+}$ at 1768 nm (1000). Using the simple equation (4) derived by

$$\Delta\nu_{1/2} = (2310\nu_{max})^{1/2} \quad (4)$$

Hush for class II mixed-valence compounds to calculate the bandwidths from the absorption maxima, we found that the observed bandwidths for [**1**]$^{\bullet+}$ and [**4**]$^{\bullet+}$ are far too small (Table 3) to account for IVCT transitions. Assuming that these species belong to class II,[2c,k] the observed bandwidths should be in good agreement with the calculated values or larger. In view of the small K_C value, an assignment for class III, which would agree with the narrow bands, is rather unlikely for these two present species.[8b,d]

The long-wavelength bands for [**2**]$^{\bullet+}$ and [**5**]$^{\bullet+}$ also cannot be assigned to an IVCT, since the observed intensities are too high for such weakly coupled systems (as assumed from electrochemistry), although the calculated and observed band-

(23) Barlow, S.; Bunting, H. E.; Ringham, C.; Green, J. C.; Bublitz, G. U.; Boxer, S. G.; Perry, J. W.; Marder, S. R. *J. Am. Chem. Soc*. **1999**, *121*, 3715−3723.

(24) Duggan, D. M.; Hendrickson, D. H. *Inorg. Chem*. **1975**, *5*, 955−970.

Table 3. K_C Values, Long-Wavelength Band Energies, and Related Data

compd[a]	K_C[b]	ν_{max} (cm^{-1})	ϵ_{max} ($M^{-1}\,cm^{-1}$)	$\Delta\nu_{1/2}^{obsd}$ (cm^{-1})	$\Delta\nu_{1/2}^{calcd}$ (cm^{-1})[c]
$[\mathbf{1}]^{\bullet+}$	6.0×10^5	6495	5820	1230	3873
$[\mathbf{4}]^{\bullet+}$	147.7	6510	630	1660	3878
$[\mathbf{2}]^{\bullet+}$	10.8	5882	230	3860	3686
$[\mathbf{5}]^{\bullet+}$	7	5656	100	4362	3614

[a] Generated by electrolysis in 0.1M $^nBu_4NPF_6/CH_2Cl_2$ solution. [b] From eq 1. [c] From eq 4.

widths are in better agreement. A closer inspection of the band maxima and band shape reveals that the spectra of $[\mathbf{1}]^{\bullet+}$ and $[\mathbf{4}]^{\bullet+}$ are very similar. The same holds for $[\mathbf{2}]^{\bullet+}$ and $[\mathbf{5}]^{\bullet+}$. Furthermore, it seems that upon the second oxidation the long-wavelength bands for [**1**] and [**4**] do not disappear but shift to higher energies (Figure 1, right). Thus, an IVCT assignment for the long-wavelength bands of the mixed-valence states is doubtful, although at least for $[\mathbf{1}]^{\bullet+}$ an IVCT band should be observable.

An alternative assignment for the long-wavelength absorption bands would be intraligand transitions (IL) arising from the partially emptied HOMO. Recent quantum-chemical calculations have shown that the HOMO in such complexes obtains strong to main contributions from ligand π orbitals.[2b,3,5d,8d,20−22] Upon oxidation of the complexes additional transitions are possible to HOMO → SOMO and from, for example, SOMO → LUMO, the singly occupied molecular orbital (SOMO). Such intraligand transitions should be weak (symmetry forbidden), might be partially structured due to phonon coupling (mainly $\nu_{C\equiv C}$), and should occur in the low-energy range of the spectrum (close-lying π and π^* orbitals). Such transitions have been observed frequently, e.g. for singly reduced aromatic and heteroaromatic ligand systems.[25] Thus, the partially structured long-wavelength bands around 1700 nm (7000 cm^{-1}) might be assigned to a HOMO → SOMO transition and the structured band systems around 500 nm (20 000 cm^{-1}) to a SOMO → LUMO transition. This assignment would be in line with the above-described similarities of $[\mathbf{1}]^{\bullet+}$ and $[\mathbf{4}]^{\bullet+}$ vs $[\mathbf{2}]^{\bullet+}$ and $[\mathbf{5}]^{\bullet+}$.

Further support for this assignment comes from the spectral response of the oxidation of **3** to $[\mathbf{3}]^{2+}$ (Figure 3), which is comparable to the spectra obtained for the second oxidation of **1**, **2**, or **4**. The spectra are characterized by weak to medium structured bands around 1000 nm which do not look very different from the bands observed for the monocations $[\mathbf{1}]^{\bullet+}$, $[\mathbf{2}]^{\bullet+}$, or $[\mathbf{4}]^{\bullet+}$, although they are markedly blue-shifted.

Even upon careful and partial oxidation of **3** there was no evidence for long-wavelength bands which would correspond to $[\mathbf{3}]^{\bullet+}$. This supports our conclusions from CV measurements that there is no connection between the two ruthenium sites and they are both oxidized independently at the same potential. Further oxidation of $[\mathbf{5}]^{\bullet+}$ to $[\mathbf{5}]^{3+}$ leads to the same state as for $[\mathbf{1}]^{2+}$−$[\mathbf{4}]^{2+}$, all with formally fully oxidized ruthenium centers.

Assuming contributions of the bridge to the former HOMO, an assignment for the observed bands has to consider the metallacumulene type of structure shown in Scheme 3.[8d,9a] On the basis of recent work on related Ru−allenylidene complexes,

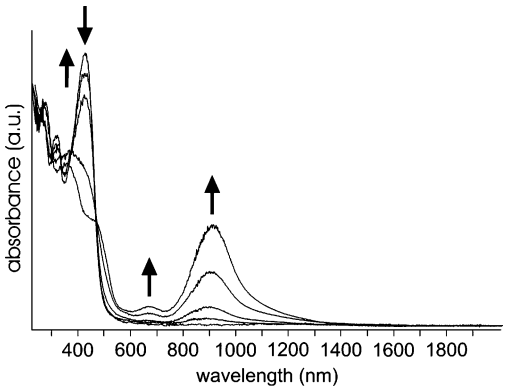

Figure 3. Absorption spectra of [**3**] taken during the electrochemical oxidation in THF/$^nBu_4NPF_6$.

Scheme 3. Oxidation of 3 to the Allenylidene Complex $[3]^{2+}$

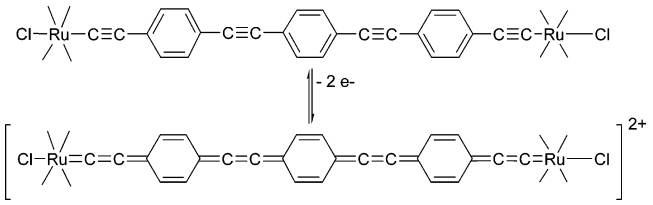

we assign the intense long-wavelength bands between 800 and 1000 nm to mixed $\pi_{ligand}/d_{Ru} \rightarrow \pi^*_{ligand}$ (IL/MLCT) transitions.[20] The metallacumulene type of structure and thus the contribution of the alkynyl ligand to the oxidation will be further substantiated by vibrational spectroscopy (vide infra).

The spectra obtained upon oxidation of the ferrocenyl derivatives does not indicate any occurrence of mixed-valence species. The observed long-wavelength absorption bands at 800 and 900 nm respectively correspond to the dications $[\mathbf{6}]^{2+}$ and $[\mathbf{7}]^{2+}$ and can be also observed upon oxidation of ferrocene (λ_{max} 617 nm). Due to the much weaker connection between the metal and alkynyl bridge we assume here far more metal-centered oxidations and tentatively assign these transitions to ligand (Cp) to metal (Fe(III)) charge transfer (LMCT) or, rather, to ligand field transitions due to their weakness.[24]

IR Spectroelectrochemistry. IR spectroelectrochemistry was performed in the range from 7000 to 900 cm^{-1}, which has enabled us not only to probe for vibrational responses to electrochemical oxidation but also to confirm the long-wavelength bands detected in the UV/vis/near-IR spectra. The IR spectra of the parent complexes are characterized among others by strong bands between 2060 and 2070 cm^{-1}. They are assigned to the symmetric $\nu_{C\equiv C}$ stretch (Table 4). The frequency does not depend much on the character of the complexes, and a comparison between **2** and **3** reveals that the frequency does not depend at all on the chain length.

Complex **3** is not expected to give a mixed-valence species, and upon oxidation the original band at 2061 cm^{-1} bleaches and a new band at 1902 cm^{-1} appears (shift $\Delta = 159$ cm^{-1}). If the character of the starting systems can be described as arylethynyl with triple bonds for the C≡C group, these spectral changes for the resulting Ru(III)/Ru(III) dication $[\mathbf{3}]^{2+}$ are in line with an allenylic type of description as shown in Scheme 3. Support for this assignment comes from two further bands of medium intensity at 1592 and 1515 cm^{-1} that disappear upon oxidation and one broad and strong band at 1568 cm^{-1} which appears. The two bands in the starting material can be assigned to the aromatic C−C bonds in the central and peripheral phenyl units. The oxidation renders these phenyl moieties more similar

(25) (a) Chanda, N.; Sarkar, B.; Fiedler, J.; Kaim, W.; Lahiri, G. K. *Dalton Trans.* **2003**, 3550−3555. (b) Klein, A.; McInnes, E. J. L.; Kaim, W. *Dalton Trans.* **2002**, 2371−2378. (c) Klein, A. *Rev. Inorg. Chem.* **2001**, *20*, 283−303. (d) Adams, C. J.; James, S. L.; Liu, X.; Raithby, P. R.; Yellowlees, L. J. *Dalton Trans.* **2000**, 63−67. (e) Fletcher, N. C.; Robinson, T. C.; Behrendt, A.; Jeffrey, J. C.; Reeves, Z. R.; Ward, M. D. *J. Chem. Soc., Dalton Trans.* **1999**, 2999−3006. (f) Collison, D.; Mabbs, F. E.; McInnes, E. J. L.; Taylor, K. J.; Welch, A. J.: Yellowlees, L. J. *J. Chem. Soc., Dalton Trans.* **1996**, 329−334.

Table 4. Selected IR Frequencies (cm^{-1}) of Binuclear Ruthenium and Iron Complexes[a]

	$n = 0$	$n = 1$			$n = 2$			$n = 3$
[**1**]^n	2071 s	2068 m	1966 vs	1570 s	1918 s			
[**2**]^n	2062 s	2046 s, 2025 s	1975 s, 1907 s	1555 s	1907 s	1572 s		
[**3**]^n	2061 vs				1902 vs	1568 vs		
[**4**]^n	2069 vs	2067 vs	1967 vs	1567 s	1915 s	1560 vs		
[**5**]^n	2058 s	2038 s, 2024 s	1978 s, 1892 vs	1556 vs				1892 vs
[**6**]^n	2205 vs				2205 vs			2210 vs
[**7**]^n	2095 vs				2202 vs, 2093 vs	1594 s	1510 s	2208 m, 2125 m

[a] Generated by electrolysis in 0.1M ^{n}Bu$_4$NPF$_6$/CH_2Cl_2 solution; assigned to $\nu_{C\equiv C}$ or $\nu_{C=C}$ resonances.

Scheme 4. Valence Structures of [1], [1]•$^+$, and [1]$^{2+}$

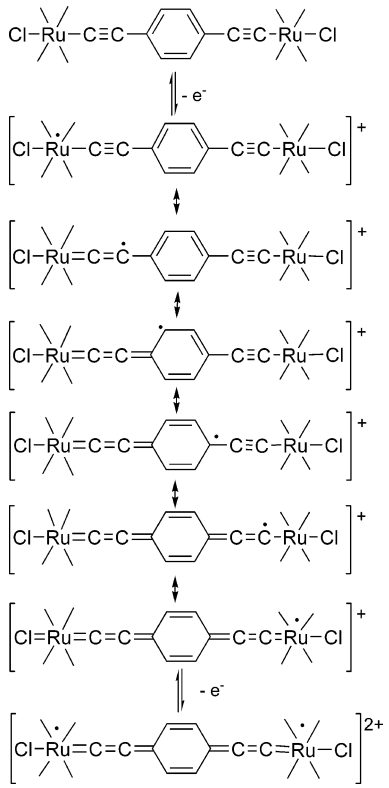

in character, and thus they give only one (broad) resonance. For the ferrocenyl derivatives **6** and **7** a similar behavior is observed.

Upon oxidation of **1** the band at 2071 cm^{-1} decreases; at the same time a very strong band at 1966 cm^{-1} appears ($\Delta = 104$ cm^{-1}). Even after exhaustive oxidation still some residual band is observed at 2068 cm^{-1} (slightly less than half of the original intensity). If the mixed-valence species [**1**]$^+$ were a fully delocalized system, the original band should disappear.[2k,8b,d] The residual band could mean that the system is not fully delocalized on the IR time scale, which is in line with a valence-trapped class II system.[8d] Further strong bands are found at 1570 and 965 cm^{-1}. The first might either be assigned to a C−C stretch vibration in the phenyl ring that has lost some of its double-bond character and gained some intensity due to higher distortion or assigned to a C−C stretching vibration that has gained some double-bond character (see Scheme 4). Upon further oxidation the band at 1966 cm^{-1} bleaches and a band at 1918 cm^{-1} ($\Delta = 152$ cm^{-1}) of middle to weak intensity appears. Complexes **2**, **4**, and **5** show behavior quite similar to that discussed for **1**.

To conclude for the IR spectroelectrochemistry, the large shift of the C≡C stretching mode upon oxidation for the ruthenium complexes supports the assumption that the bridging ligand is largely involved in the molecular orbitals relevant for the oxidation. Further support should come from a closer inspection of the character of the SOMO in the mono-oxidized complexes using EPR spectroscopy.

Table 5. EPR Data of Ruthenium and Iron Complexes[a]

	solvent	g_{iso} (298 K)	g_1	g_2	g_3	T (K)	$\langle g_{calcd}\rangle$	Δg
[**1**]•$^+$	THF	2.0469	2.155	2.052	1.992	110	2.067	0.163
[**1**]•$^+$	CH_2Cl_2		2.1582	2,0520	1.9923	3.2	2.068	0.166
[**2**]$^{2+}$	CH_2Cl_2		2.3705	2.0953	2.0706	3.4	2.183	0.300
[**3**]$^{2+}$	THF		2.228	2.042	1.914	110	2.065	0.314
[**4**]•$^+$	THF		2.154	2.053	1.996	3.4	2.068	0.158
[**4**]$^{2+}$	THF		2.316	2.049	1.956	3.4	2.112	0.360
[**5**]$^{3+}$	CH_2Cl_2		2.3232	2.0546	1.9481	3.4	2.114	0.375
[**7**]$^{2+}$	THF		4.14	1.58	1.58	3.4	2.71	2.56

[a] Generated by electrolysis in 0.1M ^{n}Bu$_4$NPF$_6$/solvent solution; g values were extracted from spectral simulation assuming a Gaussian line form (see, for example, Figure 4).

EPR Spectroelectrochemistry. The monocationic species generated upon the first oxidation should be paramagnetic. The dicationic systems might either represent a configuration with two unpaired electrons for mainly metal-centered oxidations and no coupling or could be diamagnetic due to coupling phenomena or essentially ligand-centered oxidation. The oxidized species have been generated by in situ electrolysis and studied in glassy frozen solutions at low temperature since, with the exception of [**1**]•$^+$ which could be also detected at 298 K in fluid solution, they were EPR silent at ambient temperature (see Table 5). Such EPR silence at higher temperatures is frequent for Ru(III) species and is probably due to rapid relaxation processes.[26]

For [**1**]•$^+$ at 298 K an isotropic, broad signal was found at $g = 2.047$ which did not show any hyperfine splitting (HFS). The low-temperature spectrum of [**1**]•$^+$ exhibits rhombic symmetry with no HFS. The averaged g value $\langle g_{calc}\rangle = 2.067$ fits roughly to the g_{iso} value measured at 298 K. The spectra for the other species look essentially the same (rhombic, broad, no HFS). During the oxidative electrolysis of the complexes in most cases only one type of radical species could be detected, with the exception of **4**, where two different radical species were observed (Figure 4). A closer look reveals that the observed signals fall into two categories for the ruthenium complexes. Type I shows g anisotropy (Δg) of about 0.160 and is observed for **1** and **4**. Type II species reveal Δg values between 0.300 and 0.360, which is approximately double the value found for type I. Type II is observed for **2**−**5** (see Table 5).

From these two lists we can conclude that the type I signals are due to the mixed-valence species [**1**]•$^+$ and [**4**]•$^+$, whereas the type II radicals can be assigned to the formal Ru(III)/Ru(III) dimers [**2**]$^{2+}$−[**4**]$^{2+}$ or the trimer [**5**]$^{3+}$. Prolonged oxidation of **1** to obtain [**1**]$^{2+}$ did not yield a further signal for the formed dication (down to 3.4 K). We assume antiferromagnetic coupling phenomena to be responsible for the fact

(26) Sarkar, B.; Kaim, W.; Klein, A.; Schwederski, B.; Fiedler, J.; Duboc-Toia, C.; Lahiri, G. K. *Inorg. Chem.* **2003**, *42*, 6172−6174.

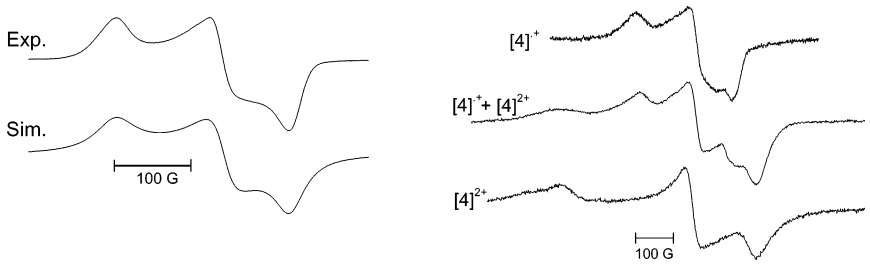

Figure 4. X-band EPR experimental (at 110 K) and simulated spectra of $[\mathbf{1}]^{\bullet+}$ (left) and experimental spectra of $[\mathbf{4}]^{\bullet+}$ and $[\mathbf{4}]^{2+}$ (at 3.4 K) (right) observed during oxidative electrolysis of **4** in THF/$^{n}Bu_4NPF_6$.

that the dicationic species $[\mathbf{1}]^{2+}$ with two formal Ru(III) centers cannot be detected by EPR. For **4** the coupling seems to be much less effective, thus allowing the observation of both $[\mathbf{4}]^{\bullet+}$ and $[\mathbf{4}]^{2+}$.

The reason why $[\mathbf{2}]^{\bullet+}$ and $[\mathbf{5}]^{\bullet+}$ could not be detected, although from the electrochemical experiments these states are accessible, might be found in their reduced stability (rapid disproportionation). Another reason might be that their signals are obscured by the stronger signals of the dications, but since the signals should occur at different frequencies (see for $[\mathbf{4}]^{\bullet+}$ and $[\mathbf{4}]^{2+}$) this is unlikely. For **3**, which does not form a monocation, the situation is clear (type II, $\Delta g = 0.314$), which confirms our assignments. EPR data of comparable ruthenium complexes have not been reported so far. Related iron butadiynyl complexes with very similar values for the mixed-valence cations have been investigated (e.g. [Cp′Fe(dppe)(μ-C_4)Cp′Fe-$(CO)_2$] (Cp′ = C_5Me_5, C_5Ph_5), with $\langle g_{calc}\rangle = 2.126$ and $\Delta g = 0.35$,[8g] and [(μ-C_4){Cp*Fe(dippe)}$_2$] (dippe = ethylenebis-(diisopropylphosphine), with $\langle g_{calc}\rangle = 2.118$ and $\Delta g = 0.25$[8g]).

From the g values, which were all markedly higher than 2.0023 (the g value for the free electron) and also from the observed relatively high g anisotropy ($\Delta g = g_1 - g_3$) an appreciable metal contribution can be inferred for all species.[27] However, they are far from being purely metal-centered Ru(III) states. Organometallic ruthenium(III) centers usually exhibit Δg values ranging between 0.3 and 0.6 with individual g components ranging from 1.5 to 2.5.[28] Thus, the species presented here are at the lower end of metal contribution. This means that the spin density of the unpaired electron(s) is distributed over the bridge and the metal centers, as exemplified in Scheme 4. An interesting phenomenon in that respect is the doubling of the g anisotropy on going from the monooxidized to the doubly oxidized species, which signifies a higher metal contribution for the latter.

For the ferrocenyl complexes only the palladium-bridged complex **7** was examined. An ESR signal was only observed at low temperatures (4 K). The signal is of axial symmetry and reveals a very high anisotropy (see Table 5). Such values are typical for ferrocenium.[24,28a,29] Therefore, and in view of our electrochemical results (no formation of the cation $[\mathbf{7}]^{\bullet+}$), we assign this signal to the dication $[\mathbf{7}]^{2+}$. The Δg value here is rather high, which is mainly due to the special symmetry and d orbital splitting for ferrocenium. In comparison to ferrocenium itself ($g_1 = 4.36$, $g_{2,3} = 1.28$; $\Delta g = 3.08$) the values for $[\mathbf{7}]^{2+}$ are smaller. Thus, there is evidence for some contribution of the alkynyl bridge, but much smaller than that observed for the ruthenium systems described above. This is in excellent agreement with our other findings (UV/vis/near-IR) and has its origin in the structure, in which the arylethynyl bridge is not connected to the metal but to one of the Cp ring carbon atoms.

Conclusion

Multiple spectroscopic, electrochemical, and spectroelectrochemical investigations have revealed the influence of the arylethynyl bridging ligand systems on the intramolecular electron transfer (ET) abilities of binuclear ruthenium or iron complexes. Taking the comproportionation constant K_C as a measure for the ET, we found that (i) upon prolongation of the carbon chain by two phenylethynyl units the ET vanished, (ii) introduction of complex metal fragments was conducive to the electron transfer, and (iii) the coordination mode of the arylethynyl bridge to the metal (directly or via a ligand) is crucial for the ET.

However, the role of the arylethynyl bridge is not solely restricted to mediate electronic coupling between the metal redox centers. Mainly from EPR spectroscopy we can conclude strong contributions of the bridging ligand to the HOMO (target orbital for the oxidation) for the ruthenium systems and much reduced contributions of the ligands for the ferrocenium complexes. As a result, the long-wavelength absorption bands of the parent complexes are assigned to transitions with appreciable ligand contributions (IL/MLCT). For the monooxidized ruthenium complexes the IVCT transitions cannot be assigned unequivocally; thus, the long-wavelength absorptions might as well be attributed to HOMO → SOMO and SOMO → LUMO intraligand transitions.

Experimental Section

Instrumentation. NMR spectra were recorded using a Bruker DPX 200 instrument operating at 200.131 MHz for ^{1}H spectra and at 81.014 MHz for ^{31}P spectra or on a Bruker AC 300 P instrument operating at 300.134 MHz for ^{1}H spectra and at 121.496 MHz for ^{31}P spectra. ^{31}P chemical shifts are relative to external H_3PO_4 (85%). Microanalyses results were obtained via the Service Centrale d'Analyse, CNRS, Vernaison, France. HRMS measurements were obtained with a ZabSpec TOF Micromass instrument (Centre Régional de Mesures Physiques de l'Ouest, Rennes, France). Cyclic voltammetry was carried out at a 100 mV/s scan rate in 0.1 M $^{n}Bu_4NPF_6$ solutions using a three-electrode configuration (glassy-carbon electrode, Pt counter electrode, Ag/AgCl reference) and a PAR 273 potentiostat and function generator. The ferrocene/ferrocenium couple served as an internal reference. Spectroelectrochemical measurements (in 0.1 M $^{n}Bu_4NPF_6$ solutions) were performed using an optically transparent thin-layer electrode

(27) (a) Patra, S.; Sarkar, B.; Ghumaan, S.; Fiedler, J.; Kaim, W.; Lahiri, G. K. *Dalton Trans.* **2004**, 754−758. (b) Patra, S.; Sarkar, B.; Ghumaan, S.; Fiedler, J.; Záli×f0, S.; Kaim, W.; Lahiri, G. K. *Dalton Trans*. **2004**, 750−753. (c) Klein, A.; McInnes, E. J. L.; Scheiring, T.; Záli×f0, S. *J. Chem. Soc., Faraday Trans.* **1998**, 2979−2984.

(28) (a) Sixt, T.; Fiedler, J.; Kaim, W. *Inorg. Chem. Commun*. **2000**, *3*, 80−82. (b) Winter, R. F.; Hornung, F. M. *Organometallics* **1999**, *18*, 4005−4014.

(29) (a) Elschenbroich, C.; Bilger, E.; Ernst, R. D.; Wilson, D. R.; Kralik, M. S. *Organometallics* **1985**, *4*, 2068−2071. (b) Prins, R.; Kortbeek, A. G. T. G. *J. Organomet. Chem*. **1971**, *33*, C33−C34. (c) Prins, R.; Korswagen, A. R. *J. Organomet. Chem*. **1970**, *25*, C74−C76. (d) Prins, R.; Reinders, F. J. *J. Am. Chem. Soc.* **1969**, *91*, 4929−4931.

(OTTLE) cell[30] for UV/vis/near-IR spectra and a two-electrode capillary for EPR studies. IR spectra were recorded on a Perkin-Elmer FT-IR PARAGON 1000 PC spectrometer. UV/vis/near-IR absorption spectra were recorded on a Bruins Instruments Omega 10 spectrophotometer. EPR spectra were recorded in the X band on a Bruker System ESP 300 equipped with a Bruker ER035M gauss meter and a HP 5350B microwave counter. Spectral simulation was performed using Bruker SimFonia V1.25 using Gaussian line shapes.

Preparation of the Compounds. Commercially available reagents from Aldrich or Acros were used without further purification. Solvents were dried by standard procedures. All reactions involving metal complexes were conducted under nitrogen by standard Schlenk techniques. The synthesis of **1**, **4**, **6**, **7**, and $\mathbf{P_4}$,[4g] of $\mathbf{P_7}$ and $\mathbf{P_8}$,[6j] of $\mathbf{P_3}$,[31] and of $\mathbf{P_5}$ and $\mathbf{P_6}$[32] were performed as previously described.

[Cl(dppe)$_2$Ru−(C≡CC$_6$H$_4$)$_2$−C≡C−Ru(dppe)$_2$Cl] (2). Complex $\mathbf{P_1}$ (200 mg, 0.172 mmol) and complex $\mathbf{P_4}$ (184 mg, 0.172 mmol) were stirred in THF (10 mL) and N^{i}Pr$_2$H (2 mL) for 24 h in the presence of [PdCl$_2$(PPh$_3$)$_2$] (6 mg, 9×10^{-3} mmol) and CuI (2 mg, 9×10^{-3} mmol). The color of the heterogeneous mixture turned from yellow to yellow-orange. After the solvent was removed, the yellow-orange solid was washed sequentially with water (3 × 20 mL), EtOH (3 × 20 mL), and pentane (3 × 20 mL) to give a yellow-orange solid. This was washed with a minimum amount of THF to give pure **2**. Yield: 0.23 g (64%). Anal. Calcd for $C_{122}H_{104}P_8Cl_2Ru_2$: C, 70.08; H, 5.01. Found: C, 70.10; H, 4.99. ^{1}H NMR (200 MHz, $CDCl_3$, 297 K; δ (ppm)): 7.6−6.4 (m, C_6H_5 and C_6H_4), 2.70 (broad s, CH_2CH_2). ^{31}P NMR (81.014 MHz, $CDCl_3$, 297 K; δ (ppm)): 49.57. IR (KBr; cm^{-1},): 2058 (ν_{CCRu}); no signal at 3223 corresponding to CC−H was detected.

[Cl(dppe)$_2$Ru−(C≡CC$_6$H$_4$)$_3$−C≡C−Ru(dppe)$_2$Cl] (3). Complex $\mathbf{P_1}$ (700 mg, 0.6 mmol) and 1,4-diethynylbenzene ($\mathbf{P_5}$; 38 mg, 0.3 mmol) were stirred in THF (10 mL) and N^{i}Pr$_2$H (4 mL) for 18 h in the presence of [PdCl$_2$(PPh$_3$)$_2$] (21 mg, 0.03 mmol) and CuI (6 mg, 0.03 mmol). The heterogeneous mixture turned from orange-yellow to yellow. After the solvent was removed, the yellow solid was washed sequentially with water (3 × 10 mL), EtOH (3 × 10 mL), and pentane (3 × 10 mL) to give **3** as a yellow solid. Yield: 0.64 g (95%). HRMS (*m*/*z*): calcd for [M − Cl]$^{\bullet+}$ ($C_{130}H_{108}P_8{}^{35}Cl^{102}Ru_2$), 2155.4128; found 2155.4270. Anal. Calcd for $C_{130}H_{108}P_8Cl_2Ru_2$: C, 71.1; H, 5.14. Found: C, 70.16; H, 5.08. ^{1}H NMR (200 MHz, $CDCl_3$, 297 K; δ (ppm)): 7.5−6.4 (m, C_6H_5 and C_6H_4), 2.60 (broad s, CH_2CH_2). ^{31}P NMR (81.014 MHz, $CDCl_3$, 297 K; δ (ppm)): 50.41. IR (KBr; cm^{-1}): 2055 (ν_{CCRu}), 2200 (ν_{CC}), no signal at 3223 corresponding to CC−H was detected.

[Cl(dppe)$_2$Ru−(C≡CC$_6$H$_4$)$_2$−C≡C−(dppe)$_2$Ru−(C≡CC$_6$H$_4$)$_2$−C≡C−Ru(dppe)$_2$Cl] (5). Complex $\mathbf{P_1}$ (679 mg, 0.58 mmol) and $\mathbf{P_7}$ (336 mg, 0.29 mmol) were stirred in THF (10 mL) and N^{i}Pr$_2$H (4 mL) for 18 h in the presence of [PdCl$_2$(PPh$_3$)$_2$] (21 mg, 0.03 mmol) and CuI (6 mg, 0.03 mmol). The heterogeneous mixture was yellow. After the solvent was removed, the yellow solid was washed sequentially with water (3 × 10 mL), EtOH (3 × 10 mL), and pentane (4 × 20 mL) to give **5** as a yellow solid. Yield: 0.852 g (91%). Anal. Calcd for $C_{192}H_{160}P_{12}Cl_2Ru_3$: C, 71.7; H, 5.02. Found: C, 71.23; H, 5.00. ^{1}H NMR (200 MHz, $CDCl_3$, 297 K; δ (ppm)): 7.8−6.7 (m, C_6H_5 and C_6H_4), 2.50 (broad s, CH_2CH_2). ^{31}P NMR (81.014 MHz, $CDCl_3$, 297 K; δ (ppm)): 54.72 (internal P) and 50.58 (external P). IR (KBr; cm^{-1}): 2050 (ν_{CCRu}), no signal at 3223 corresponding to CC−H was detected.

[Cl(dppe)$_2$Ru−C≡C−C$_6$H$_4$I] ($\mathbf{P_1}$). *cis*-[RuCl$_2$(dppe)$_2$] (1.479 g, 1.53 mmol) and *p*-iodoethynylbenzene ($\mathbf{P_3}$; 524 mg, 2.3 mmol) were stirred in CH_2Cl_2 (30 mL) for 16 h in the presence of $NaPF_6$ (378 mg, 2.2 mmol). After filtration the solvent was removed. The resulting green solid was carefully washed with pentane (3 × 10 mL) before addition of a mixture of 30 mL of THF and 2 mL of NEt_3. After 4 h solvents were removed and the yellow solid was washed sequentially with water (3 × 20 mL), EtOH (2 × 20 mL), and pentane (3 × 20 mL) to give $\mathbf{P_1}$ as a yellow solid. Yield: 1.54 g (87%). HRMS (*m*/*z*): calcd for [M]$^{\bullet+}$ ($C_{60}H_{52}P_4{}^{35}Cl^{102}RuI$), 1160.0796; found, 1160.0833. Anal. Calcd for $C_{60}H_{52}P_4ClRuI$: C, 62.06; H, 4.52; P, 10.68. Found: C, 62.07; H, 4.52; P, 10.00. ^{1}H NMR (300 MHz, $CDCl_3$, 297 K; δ (ppm)): 7.5−6.3 (m, C_6H_5 and C_6H_4), 2.65 (broad s, CH_2CH_2). ^{31}P NMR (121.496 MHz, $CDCl_3$, 297 K; δ (ppm)): 49.94. IR (KBr; cm^{-1}): 2064 (ν_{CCRu}).

[(dppe)$_2$Ru(−C≡CC$_6$H$_4$I)$_2$] ($\mathbf{P_2}$). *cis*-[RuCl$_2$(dppe)$_2$] (0.726 g, 0.75 mmol) and *p*-iodoethynylbenzene ($\mathbf{P_3}$; 505 mg, 2.25 mmol) were stirred in CH_2Cl_2 (22 mL) for 39 h in the presence of $NaPF_6$ (378 mg, 2.2 mmol) and NEt_3 (1.5 mL, 11.25 mmol). After the solvents were removed, the yellow solid was washed sequentially with pentane (4 × 20 mL), water (2 × 20 mL), and EtOH (2 × 20 mL) and quickly with CH_2Cl_2 (2 × 2 mL) to give $\mathbf{P_2}$ as a pale yellow solid. Yield: 0.882 g (87%). Anal. Calcd for $C_{68}H_{56}P_4RuI_2$: C, 60.41; H, 4.18; P, 9.10. Found: C, 60.01; H, 4.20; P, 10.07. ^{1}H NMR (200 MHz, $CDCl_3$, 297 K): δ (ppm) 7.4−6.4 (m, C_6H_5 and C_6H_4), 2.58 (broad s, CH_2CH_2). ^{31}P NMR (81.014 MHz, $CDCl_3$, 297 K; δ (ppm)): 53.98. IR (KBr; cm^{-1}): 2059 (ν_{CCRu}).

Acknowledgment. Prof. Dr. P. Dixneuf (Université de Rennes) and Dr. Rainer Winter (University of Stuttgart) are thanked for fruitful discussions. Dr. M. Wanner (University of Stuttgart) is acknowledged for EPR simulations.

OM050876K

(30) Krejcik, M.; Danek, M.; Hartl, F. *J. Electroanal. Chem.* **1991**, *317*, 179−187.

(31) Lavastre, O.; Ollivier, L.; Dixneuf, P. H.; Sinbandhit, S. *Tetrahedron* **1996**, *52*, 5495−5504.

(32) Lavastre, O.; Cabioch, S.; Dixneuf, P. H.; Vohlidal, J. *Tetrahedron* **1997**, *53*, 7595−7604.